

# Validation of the ASVDADD Constraint Selection Algorithm for Effective RCCE Modeling of Natural Gas Ignition in Air

**Luca Rivadossi**

Department of Mechanical and Industrial Engineering, Università di Brescia, Via Branze 38, Brescia 25123, Italy

**Gian Paolo Beretta**

Department of Mechanical and Industrial Engineering, Università di Brescia, Via Branze 38, Brescia 25123, Italy

*The rate-controlled constrained-equilibrium (RCCE) model reduction scheme for chemical kinetics provides acceptable accuracies in predicting hydrocarbon ignition delays by solving a smaller number of differential equations than the number of species in the underlying detailed kinetic model (DKM). To yield good approximations, the method requires accurate identification of the rate controlling constraints. Until recently, a drawback of the RCCE scheme has been the absence of a systematic procedure capable of identifying optimal constraints for a given range of thermodynamic conditions and a required level of approximation. A recent methodology has proposed for such identification an algorithm based on a simple algebraic analysis of the results of a preliminary simulation of the underlying DKM, focused on the degrees of disequilibrium (DoD) of the individual chemical reactions. It is based on computing an approximate singular value decomposition of the actual degrees of disequilibrium (ASVDADD) obtained from the DKM simulation. The effectiveness and robustness of the method have been demonstrated for methane/oxygen ignition by considering a C1/H/O (29 species/133 reactions) sub-mechanism of the GRI-Mech 3.0 scheme and comparing the results of a DKM simulation with those of RCCE simulations based on increasing numbers of ASVDADD constraints. Here, we demonstrate the new method for shock-tube ignition of a natural gas/air mixture, with higher hydrocarbons approximately represented by propane according to the full (53 species/325 reactions) GRI-Mech 3.0 scheme including NO<sub>x</sub> formation.*

[DOI: 10.1115/1.4038376]

## 1 Introduction

In the framework of modeling the ignition of a homogeneous methane/air mixture, the purpose of this paper is to present a validation of the recently proposed [1] approximate singular value decomposition of the actual degrees of disequilibrium (ASVDADD) method for automatic constraint selection for use in the rate-controlled constrained-equilibrium (RCCE) method of model order reduction [2–14]. The ASVDADD method requires a preliminary full detailed kinetic model (DKM) simulation aimed at computing the time dependence of the degree of disequilibrium (DoD) of every individual chemical reaction in the scheme. It then extracts the selection of RCCE constraints from the singular value decomposition (SVD) of a matrix that contains the information about the DoD-time traces of all reactions.

In Sec. 2, we review the assumptions of a typical DKM for gas-phase combustion. In Sec. 3, we recall the meaning of DoD-time trace analysis. In Sec. 4, we review the RCCE fundamentals. In Sec. 5, we outline the general logic of automatic constraint selection and in Sec. 6, we discuss the particular logic of the ASVDADD algorithm based on DoD analysis. In Sec. 7, we present the results of the numerical validation and in Sec. 8 our conclusions.

## 2 Standard Detailed Kinetic Model Formulation

A detailed kinetic model for gas-phase combustion is typically defined by:

- A list of  $n_s$  chemical species.

- A kinetic scheme with  $n_r$  chemical reactions (we denote the forward and reverse stoichiometric coefficients of the  $\ell$ th reaction by  $\nu_{j\ell}^+$  and  $\nu_{j\ell}^-$ , respectively).
- The kinetic parameters that determine the forward reaction rate constants

$$k_{\ell}^+(T) = A_{\ell}^+ T^{b_{\ell}^+} \exp(-E_{\ell}^+/RT) \quad (1)$$

(typically in mol cm s K units with the forward activation energy  $E_{\ell}^+$  in cal/mol).

- The principle of detailed balance to determine the backward reaction rate constants according to

$$k_{\ell}^-(T) = k_{\ell}^+(T)/K_{\ell}^{\text{co}}(T) \quad (2)$$

where the equilibrium constant based on concentrations is

$$K_{\ell}^{\text{co}}(T) = (p_o/RT)^{\nu_{\ell}} \exp(-\Delta g_{\ell}^o(T)/RT) \quad (3)$$

where  $\nu_{\ell} = \sum_j (\nu_{j\ell}^- - \nu_{j\ell}^+)$  and  $\Delta g_{\ell}^o(T) = \sum_{j=1}^{n_s} \nu_{j\ell} g_{jj}(T, p_o)$  is the Gibbs free energy of the  $\ell$ th reaction at standard pressure  $p_o$  and temperature  $T$ . In the present paper, we use the notation of Ref. [11], which differs only slightly from that of Ref. [15], whereby  $g_{jj} = \mu_{jj}$  (with the double subscript) refers to the Gibbs free energy of pure substance  $j$ , whereas the symbol  $g_j = \mu_j$  (with a single subscript), used below, represents instead the partial Gibbs free energy, i.e., the chemical potential, of species  $j$  in the mixture.

- The relation

$$r_{\ell}^{\pm} = k_{\ell}^{\pm}(T) \prod_{j=1}^{n_s} [N_j]^{\nu_{j\ell}^{\pm}} \quad (4)$$

Contributed by the Advanced Energy Systems Division of ASME for publication in the JOURNAL OF ENERGY RESOURCES TECHNOLOGY. Manuscript received September 19, 2017; final manuscript received September 20, 2017; published online November 30, 2017. Editor: Hameed Metghalchi.

was used to compute the forward and reverse reaction rates,  $r_\ell^+$  and  $r_\ell^-$ , respectively, where  $[N_j]$  is the concentration of species  $j$ . From these we compute the chemical production density terms in the species balance equations (consumption density if negative)

$$\dot{\omega}_j = \sum_{\ell=1}^{n_r} \nu_{j\ell} (r_\ell^+ - r_\ell^-) \quad (5)$$

and the chemical contribution to the entropy production density

$$\sigma_{\text{chem}} = R \sum_{\ell=1}^{n_r} (r_\ell^+ - r_\ell^-) \ln(r_\ell^+ / r_\ell^-) \quad (6)$$

— The local equilibrium assumption whereby the so-called “surrogate system” [16,17] obtained by instantaneously “freezing” all reactions can be assumed to have the properties of a stable thermodynamic equilibrium at temperature  $T$  and pressure  $p$  of the nonreacting mixture (hence the “off” subscript, below) with mole fractions

$$X_j = [N_j]/[N], \text{ where } [N] = \sum_{j=1}^{n_s} [N_j] \quad (7)$$

For convenience, we introduce the vector of mole fractions

$$\mathbf{X} = [X_1 \dots X_{n_s}] \quad (8)$$

— The assumption of ideal Gibbs–Dalton mixture of ideal gases whereby  $p = [N]RT$  and the chemical potential of species  $j$  in the surrogate system is given by

$$\mu_{j,\text{off}}(T, p, \mathbf{X}) = g_{ij}(T, p_o) + RT \ln(p/p_o) + RT \ln(X_j) \quad (9)$$

For convenience, we introduce the *entropic chemical potentials*

$$\lambda_j = \lambda_{j,\text{off}}(T, p, \mathbf{X}) = -\mu_{j,\text{off}}(T, p, \mathbf{X})/RT \quad (10)$$

and, for shorthand, the vectors

$$\mathbf{A} = [\lambda_1 \dots \lambda_{n_s}] \quad (11)$$

$$\mathbf{A}_{\text{pure}} = [\lambda_{11} \dots \lambda_{n_s n_s}] \quad (12)$$

$$\ln \mathbf{X} = [\ln X_1 \dots \ln X_{n_s}] \quad (13)$$

so that Eq. (9) rewrites in either of the following forms:

$$\mathbf{A} = \mathbf{A}_{\text{pure}}(T, p_o) - \ln(p/p_o) - \ln \mathbf{X} \quad (14)$$

$$\mathbf{A} = \mathbf{A}_{\text{pure}}(T, p) - \ln \mathbf{X} \quad (15)$$

### 3 Degrees of Disequilibrium

The DoD of reaction  $\ell$  is defined as

$$\phi_\ell = \ln(r_\ell^+ / r_\ell^-) \quad (16)$$

For convenience of discussion, below we refer to the degree of disequilibrium of reaction  $\ell$  also by  $\text{DoD}_\ell$ . Under the set of assumptions outlined in Sec. 2, it is easy to verify that  $\text{DoD}_\ell$  is related to  $T, p, \mathbf{X}$  via the equation

$$\phi_\ell = \sum_{j=1}^{n_s} \nu_{j\ell} \lambda_{j,\text{off}}(T, p, \mathbf{X}) \quad (17)$$

and to  $T, [N]$  via the nonequilibrium law of mass action

$$\prod_{j=1}^{n_s} [N_j]^{\nu_{j\ell}} = K_\ell^{\text{co}}(T) \exp(-\phi_\ell) \quad (18)$$

In view of Eq. (4), some DoDs are  $\pm\infty$  when some of the  $[N_j]$ 's are zero. We exclude such cases from our treatment, meaning that

for all practical purposes, when the concentration of a species  $j$  is initially zero, we substitute the zero with a very small value, like  $[N_j] = 10^{-10}[N]$ .

The mathematical interpretation of Eq. (17) is that the DoD of a reaction is a linear combination of the rows of the stoichiometric matrix, with the  $\lambda_{j,\text{off}}$ 's as coefficients of the linear combination. Thus, if some columns of the stoichiometric matrix are linearly dependent, then so are the corresponding DoDs.

We also observe that Eq. (17) may be rewritten as the scalar product of the vector  $\mathbf{A}$  with the vector

$$\mathbf{v}_\ell = [\nu_{1\ell} \dots \nu_{n_s \ell}] \quad (19)$$

whose entries correspond to the  $\ell$ th column of the matrix  $\mathbf{v} = [\nu_{j\ell}]$  of the stoichiometric coefficients, i.e., we may write

$$\phi_\ell = \sum_{j=1}^{n_s} \lambda_j \nu_{j\ell} = \langle \mathbf{A} | \mathbf{v}_\ell \rangle \quad (20)$$

where  $\langle \mathbf{x} | \mathbf{y} \rangle = \sum_{i=1}^n x_i y_i$  denotes the scalar product of two vectors  $\mathbf{x} = [x_1 \dots x_{n_s}]$  and  $\mathbf{y} = [y_1 \dots y_{n_s}]$  in the vector space  $\mathbb{R}^{n_s}$  consisting of all ordered  $n_s$ -tuples of real numbers.

From Eq. (5) and defining the *overall production density vector*

$$\mathbf{\Omega} = [\dot{\omega}_1 \dots \dot{\omega}_{n_s}] \quad (21)$$

the entropy production density may also be written as

$$\sigma_{\text{chem}} = R \sum_{j=1}^{n_s} \lambda_j \sum_{\ell=1}^{n_r} \nu_{j\ell} (r_\ell^+ - r_\ell^-) = \langle \mathbf{A} | \mathbf{\Omega} \rangle R \quad (22)$$

In general, the reactions in a given DKM are not all independent. Element conservation requires the stoichiometric coefficients to satisfy the following  $n_{\text{el}}$  balance conditions:

$$\sum_{j=1}^{n_s} a_{ij}^{\text{EL}} \nu_{j\ell} = 0, \text{ for } i = 1, \dots, n_{\text{el}} \text{ and } \ell = 1, \dots, n_r \quad (23)$$

where of course  $a_{ij}^{\text{EL}}$  represents the number of atoms of type  $i$  in a molecule of species  $j$ . These conditions guarantee that the chemical production/consumption terms in the species balances equations satisfy the *element conservation constraints*

$$\sum_{j=1}^{n_s} a_{ij}^{\text{EL}} \dot{\omega}_j = 0 \text{ for } i = 1, \dots, n_{\text{el}} \quad (24)$$

Defining the  $n_{\text{el}}$  linearly independent vectors

$$\mathbf{a}_i^{\text{EL}} = [a_{i1}^{\text{EL}} \dots a_{in_s}^{\text{EL}}] \text{ for } i = 1, \dots, n_{\text{el}} \quad (25)$$

the stoichiometric balance conditions (23) become orthogonality conditions

$$\langle \mathbf{a}_i^{\text{EL}} | \mathbf{v}_\ell \rangle = 0 \quad (26)$$

implying that the column space  $\text{span}(\{\mathbf{v}_\ell\})$  of the stoichiometric matrix  $\mathbf{v}$ , i.e., the linear span of the set of stoichiometric vectors  $\mathbf{v}_\ell$  whose entries are given by its columns, often called the reactive subspace, is orthogonal to the  $n_{\text{el}}$ -dimensional linear span  $\text{coker}(\mathbf{v})$  of the elemental constraint vectors  $\{\mathbf{a}_i^{\text{EL}}\}$ , often called the inert subspace. This also implies that the matrix  $\mathbf{v}$  of stoichiometric coefficients has rank  $r = n_s - n_{\text{el}}$ . The reactive subspace and the inert subspace are orthogonal complements in the  $n_s$ -dimensional real vector space  $\mathbb{R}^{n_s}$ , i.e., we may write

$$\mathbb{R}^{n_s} = \text{span}(\{\mathbf{v}_\ell\}) \oplus \text{coker}(\mathbf{v}) \quad (27)$$

meaning that any vector  $\mathbf{x} = [x_1 \dots x_{n_s}]$  in  $\mathbb{R}^{n_s}$  may be decomposed as  $\mathbf{x} = \mathbf{x}_{\text{span}(\{\mathbf{v}_\ell\})} + \mathbf{x}_{\text{coker}(\mathbf{v})}$  with  $\mathbf{x}_{\text{span}(\{\mathbf{v}_\ell\})}$  in  $\text{span}(\{\mathbf{v}_\ell\})$ ,  $\mathbf{x}_{\text{coker}(\mathbf{v})}$

in  $\text{coker}(\mathbf{v})$ , and of course  $\langle \mathbf{x}_{\text{span}(\{\mathbf{v}_i\})} | \mathbf{x}_{\text{coker}(\mathbf{v})} \rangle = 0$ . Therefore, applying such decomposition to the vector  $\mathbf{A}$  we may write

$$\mathbf{A} = \mathbf{A}_{\text{DoD}} + \mathbf{A}_{\perp} \quad (28)$$

where for shorthand we introduced the notation

$$\mathbf{A}_{\text{DoD}} = \mathbf{A}_{\text{span}(\{\mathbf{v}_i\})} \text{ and } \mathbf{A}_{\perp} = \mathbf{A}_{\text{coker}(\mathbf{v})} \quad (29)$$

Clearly, Eqs. (14) and (15) rewrite as

$$\mathbf{A}_{\text{DoD}} = \mathbf{A}_{\text{pure}}(T, p_o) - \mathbf{A}_{\perp} - \ln(p/p_o) - \ln \mathbf{X} \quad (30)$$

$$\mathbf{A}_{\text{DoD}} = \mathbf{A}_{\text{pure}}(T, p) - \mathbf{A}_{\perp} - \ln \mathbf{X} \quad (31)$$

We call  $\mathbf{A}_{\text{DoD}}$  the *overall degree of disequilibrium* vector (ODOd). In general, we can write

$$\mathbf{A}_{\perp} = \sum_{i=1}^{n_{\text{el}}} \gamma_i^{\text{EL}} \mathbf{a}_i^{\text{EL}} \quad (32)$$

where as shown, for example, in the appendix of Ref. [18],  $\gamma_i^{\text{EL}} = \sum_{k=1}^{n_{\text{el}}} (A^{-1})_{ik} \langle \mathbf{A} | \mathbf{a}_k^{\text{EL}} \rangle$  with  $A^{-1}$  the inverse of the matrix with elements  $A_{ik} = \langle \mathbf{a}_i^{\text{EL}} | \mathbf{a}_k^{\text{EL}} \rangle$ . Since  $\langle \mathbf{A}_{\perp} | \mathbf{v}_{\ell} \rangle = 0$ , we can rewrite Eqs. (20) and (22) as follows:

$$\phi_{\ell} = \sum_{j=1}^{n_s} \lambda_j \nu_{j\ell} = \langle \mathbf{A}_{\text{DoD}} | \mathbf{v}_{\ell} \rangle \quad \text{for } \ell = 1, \dots, n_r \quad (33)$$

$$\sigma_{\text{chem}} = \langle \mathbf{A}_{\text{DoD}} | \boldsymbol{\Omega} \rangle R \quad (34)$$

Moreover, importantly, we can construct a (nonorthogonal) basis for the  $r$ -dimensional  $\text{span}(\{\mathbf{v}_{\ell}\})$  by choosing a subset of  $r$  linearly independent columns of the stoichiometric matrix identified by the column numbers  $\ell_k$ , for  $k = 1, \dots, r$ . With respect to this basis, we can write

$$\mathbf{A}_{\text{DoD}} = \sum_{k=1}^r \alpha_k \mathbf{v}_{\ell_k} \quad (35)$$

It is also worth noting that the component  $\mathbf{A}_{\perp}$  lies in the  $n_{\text{el}}$ -dimensional linear span of the elemental constraints and is all that remains of vector  $\mathbf{A}$  at complete chemical equilibrium where all the DoDs are zero and, therefore,  $\mathbf{A}_{\text{DoD}} = 0$ .

We now substitute Eq. (35) into Eq. (33) for  $\ell = \ell_{k'}$  to obtain

$$\phi_{k'} = \sum_{k=1}^r \alpha_k \langle \mathbf{v}_{\ell_k} | \mathbf{v}_{\ell_{k'}} \rangle \quad (36)$$

which can be viewed as a linear system of equations that we can solve for the  $\alpha_k$ 's because the  $r \times r$  matrix  $\mathbf{M}_{kk'} = \langle \mathbf{v}_{\ell_k} | \mathbf{v}_{\ell_{k'}} \rangle$  is nonsingular by virtue of the linear independence of the basis vectors  $\mathbf{v}_{\ell_k}$ . Hence, denoting its inverse by  $\mathbf{W} = \mathbf{M}^{-1}$ , we can write the solution of the system as

$$\alpha_k = \sum_{k'=1}^r \phi_{k'} \mathbf{W}_{k'k} \quad (37)$$

Substituting into Eq. (35), we obtain  $\mathbf{A}_{\text{DoD}} = \sum_{k=1}^r \sum_{k'=1}^r \phi_{k'} \mathbf{W}_{k'k} \mathbf{v}_{\ell_k} = \sum_{k=1}^r \phi_k \sum_{k'=1}^r \mathbf{W}_{kk'} \mathbf{v}_{\ell_{k'}}$  which shows that we can transform to a more convenient (still nonorthogonal) basis for  $\text{span}\{\mathbf{v}_{\ell}\}$ , defined by the transformation

$$\boldsymbol{\chi}_k = \sum_{k'=1}^r \mathbf{W}_{kk'} \mathbf{v}_{\ell_{k'}} \quad (38)$$

with respect to which the coordinates of  $\mathbf{A}_{\text{DoD}}$  are the DoD's of the chosen  $r$  linearly independent reactions  $\ell_k$ , for  $k = 1, \dots, r$ , i.e.,

$$\mathbf{A}_{\text{DoD}} = \sum_{k=1}^r \phi_k \boldsymbol{\chi}_k \quad (39)$$

It is important to note that the basis vectors  $\boldsymbol{\chi}_k$  can be computed once and for all, for the given DKM, by simple algebraic operations based exclusively on the matrix  $\mathbf{v}$  of stoichiometric coefficients. Note also that the same procedure may yield different linearly independent sets of reactions and basis vectors  $\boldsymbol{\chi}_k$  if the columns of the stoichiometric matrix are sorted in a different order.

Relation (39) is very important for the ASVDADD algorithm of automatic selection of RCCE constraints. It is also important in general for the analysis of results obtained from a DKM simulation because it allows to construct the ODOd vector  $\mathbf{A}_{\text{DoD}}$  from the values  $\phi_k$  of the DoDs of only a subset of  $r$  independent reactions.

In this paper, we consider the unsteady problem of predicting the ignition delay time of a homogeneous gas mixture. Therefore, the results of a DKM simulation will be functions of time  $t$  only, i.e., Eq. (39) is rewritten as

$$\mathbf{A}_{\text{DoD}}^{\text{DKM}}(t) = \sum_{k=1}^r \phi_k^{\text{DKM}}(t) \boldsymbol{\chi}_k \quad (40)$$

#### 4 Rate-Controlled Constrained-Equilibrium Approximation

The main assumption of the RCCE modeling approximation is that the gas mixture evolves along a low-dimensional manifold in composition space where the associated local equilibrium states of the surrogate system, i.e., the stable equilibrium state obtained by instantaneously freezing all reactions, have the *constrained-equilibrium* composition  $\mathbf{X}^{\text{CE}}$  that minimizes the Gibbs free energy for the instantaneous local values of the temperature  $T$ , the pressure  $p$ , the element concentrations  $[N_i^{\text{EL}}]$ , and a set of  $n_c (< r)$  rate-controlling constraint densities  $c_i([N])$ , defined as linear combinations of the local species concentration via the relations

$$\sum_{j=1}^{n_s} a_{ij}^{\text{EL}} [N_j] = [N_i^{\text{EL}}] \quad \text{for } i = 1, \dots, n_{\text{el}} \quad (41)$$

$$\sum_{j=1}^{n_s} a_{ij}^{\text{CE}} [N_j] = c_i([N]) \quad \text{for } i = 1, \dots, n_c \quad (42)$$

where the constraint matrix  $\mathbf{a}^{\text{CE}} = [a_{ij}^{\text{CE}}]$  plays a crucial role and must be chosen so that Eq. (42) possibly represent the slowest varying linear combinations of the local concentrations, in principle associated with the main rate-controlling bottlenecks of the underlying DKM at the local conditions. The composition  $\mathbf{X}^{\text{CE}}$  defined by such constrained minimization is

$$\ln \mathbf{X}_j^{\text{CE}} = \lambda_{jj}(T, p) - \sum_{i=1}^{n_{\text{el}}} \gamma_i^{\text{EL,CE}} a_{ij}^{\text{EL}} - \sum_{i=1}^{n_c} \gamma_i^{\text{CE}} a_{ij}^{\text{CE}} \quad (43)$$

Introducing as in Sec. 3 the following notation:

$$\mathbf{A}_{\perp}^{\text{CE}} = \sum_{i=1}^{n_{\text{el}}} \gamma_i^{\text{EL,CE}} \mathbf{a}_i^{\text{EL}} \quad (44)$$

$$\mathbf{A}_{\text{DoD}}^{\text{CE}} = \sum_{i=1}^{n_c} \gamma_i^{\text{CE}} \mathbf{a}_i^{\text{CE}} \quad (45)$$

$$\mathbf{a}_i^{\text{CE}} = [a_{i1}^{\text{CE}} \dots a_{i n_s}^{\text{CE}}] \quad \text{for } i = 1, \dots, n_c \quad (46)$$

$$\ln \mathbf{X}^{\text{CE}} = [\ln X_1^{\text{CE}} \dots \ln X_{n_s}^{\text{CE}}] \quad (47)$$

we may rewrite Eq. (43) in the following form:

$$\mathbf{A}_{\text{DoD}}^{\text{CE}} = \mathbf{A}_{\text{pure}}(T, p) - \mathbf{A}_{\perp}^{\text{CE}} - \ln \mathbf{X}^{\text{CE}} \quad (48)$$

suitable for comparison with the ODoD vector resulting from a full DKM simulation, which according to Eq. (31) is

$$\mathbf{A}_{\text{DoD}}^{\text{DKM}} = \mathbf{A}_{\text{pure}}(T, p) - \mathbf{A}_{\perp}^{\text{DKM}} - \ln \mathbf{X}^{\text{DKM}} \quad (49)$$

Subtracting these two equations, if the composition  $\mathbf{X}^{\text{CE}}$  is a good approximation of  $\mathbf{X}^{\text{DKM}}$ , we may write the following formal expression for the vector of relative errors:

$$\begin{aligned} \frac{\mathbf{X}^{\text{CE}} - \mathbf{X}^{\text{DKM}}}{\mathbf{X}^{\text{DKM}}} &\approx \ln \left( \frac{\mathbf{X}^{\text{CE}}}{\mathbf{X}^{\text{DKM}}} \right) = \mathbf{A}_{\text{DoD}}^{\text{DKM}} - \mathbf{A}_{\text{DoD}}^{\text{CE}} \\ &+ \sum_{i=1}^{n_{\text{el}}} \left( \gamma_i^{\text{EL,DKM}} - \gamma_i^{\text{EL,CE}} \right) \mathbf{a}_i^{\text{EL}} \end{aligned} \quad (50)$$

where of course we introduced the shorthand notation

$$\ln(\mathbf{X}/\mathbf{X}^{\text{CE}}) = \left[ \ln(X_1^{\text{CE}}/X_1^{\text{DKM}}) \dots \ln(X_{n_s}^{\text{CE}}/X_{n_s}^{\text{DKM}}) \right] \quad (51)$$

$$\frac{\mathbf{X}^{\text{CE}} - \mathbf{X}^{\text{DKM}}}{\mathbf{X}^{\text{DKM}}} = \left[ \frac{X_1^{\text{CE}} - X_1^{\text{DKM}}}{X_1^{\text{DKM}}} \dots \frac{X_{n_s}^{\text{CE}} - X_{n_s}^{\text{DKM}}}{X_{n_s}^{\text{DKM}}} \right] \quad (52)$$

Also, for the entropy production density the error is

$$\sigma_{\text{chem}}^{\text{CE}} - \sigma_{\text{chem}}^{\text{DKM}} = \langle \mathbf{A}_{\text{DoD}}^{\text{DKM}} - \mathbf{A}_{\text{DoD}}^{\text{CE}} | \boldsymbol{\Omega} \rangle R \quad (53)$$

## 5 Selection of Rate-Controlled Constrained-Equilibrium Constraints

The general idea behind the RCCE method [1–14] is that for each set of conditions and a given degree of acceptable approximation there is a threshold time scale which essentially separates the “relatively fast” equilibrating mechanisms from those that slow down and control the spontaneous relaxation toward stable chemical equilibrium. The “relatively slow” mechanisms control the interesting part of the nonequilibrium dynamics in that they effectively identify a low-dimensional manifold in composition space, where, for the chosen level of approximation, the dynamics can be assumed to take place. In general, as shown in Ref. [19], time-scale-based methods for the selection of constraints do not necessarily identify the most effective set of constraints, whereas it was shown in Ref. [12] that the analysis of DoD traces provides important information. Reference [1] developed the idea into a truly algorithmic method for automatic RCCE-constraint selection based on choosing, for a preset value of  $n_c$ , the  $n_c$  constraint vectors  $\mathbf{a}_i^{\text{CE}}$  that minimize a suitably weighted average of the relative error between the ODoD vector time-traces  $\mathbf{A}_{\text{DoD}}^{\text{CE}(n_c)}(t)$  and  $\mathbf{A}_{\text{DoD}}^{\text{DKM}}(t)$  obtained, respectively, from the RCCE simulation and the DKM simulation, starting from the same initial conditions.

A weighted average of the relative error may be defined as

$$\epsilon(n_c) = \frac{\int_{t_{\text{initial}}}^{t_{\text{final}}} \left| \mathbf{A}_{\text{DoD}}^{\text{DKM}}(t) - \mathbf{A}_{\text{DoD}}^{\text{CE}(n_c)}(t) \right|^2 w^2(t) dt}{\int_{t_{\text{initial}}}^{t_{\text{final}}} \left| \mathbf{A}_{\text{DoD}}^{\text{DKM}}(t) \right|^2 w^2(t) dt} \quad (54)$$

where  $|\Lambda|^2 = \sum_{j=1}^{n_s} [\Lambda_j]^2$  and the weight function  $w^2(t)$  is to be chosen so as to emphasize the important features of the time traces, in particular, where the solution varies rapidly.

A DKM or RCCE simulation requires the numerical integration of a set of (stiff) differential equations for  $T, p, \mathbf{X}$  or  $T, [\mathbf{N}]$  or  $T, p, \Lambda$ . Typically, we use a differential equation solver which chooses variable integration time steps so as to meet efficiently the prescribed error tolerances. For the homogeneous ignition problem at hand, the resulting time-discretization grid is typically a nonuniform time sequence,  $t_0 \dots t_p \dots t_P$  where the index  $p$  labels the  $P$

points and  $P$  is usually a large integer. The ODoD vector that results from such a DKM simulation is an  $n_s \times P$  matrix

$$\mathbf{A}_{\text{DoD}}^{\text{DKM}}(t_p) = \left[ \mathbf{A}_{\text{DoD},jp}^{\text{DKM}} \right] \quad (55)$$

that using Eq. (39) we can write as

$$\mathbf{A}_{\text{DoD}}^{\text{DKM}}(t_p) = \sum_{k=1}^r \phi_k^{\text{DKM}}(t_p) \boldsymbol{\chi}_k \quad (56)$$

Therefore, this  $n_s \times P$  matrix has rank  $r = n_s - n_{\text{el}}$ .

The RCCE method seeks to approximate this matrix with one of smaller rank  $n_c < r$

$$\mathbf{A}_{\text{DoD}}^{\text{CE}(n_c)}(t_p) = \sum_{i=1}^{n_c} \gamma_i^{\text{CE}}(t_p) \mathbf{a}_i^{\text{CE}} \quad (57)$$

where the constraint vectors  $\mathbf{a}_i^{\text{CE}}$  are chosen so as to minimize an error measure such as that defined in Eq. (54).

## 6 Approximate Singular Value Decomposition of the Actual Degrees of Disequilibrium Algorithm Based on Degrees of Disequilibrium Analysis of a Detailed Kinetic Model Simulation

The ASVDADD algorithm bases the selection of constraints on the [20,21] SVD of the  $n_s \times P$  matrix  $\mathbf{A}_{\text{DoD}}^{\text{DKM}}(t_p)$  obtained from a preliminary DKM simulation for the problem at hand. The canonical form of the SVD is

$$\mathbf{A}_{\text{DoD}}^{\text{DKM}}(t_p) = \mathbf{U} \boldsymbol{\Sigma} \mathbf{V}^T \quad (58)$$

The  $r = n_s - n_{\text{el}}$  nonzero singular values  $\sigma_j$  are in decreasing order in the  $n_s \times P$  diagonal matrix  $\boldsymbol{\Sigma}$  followed by the zero ones. The first  $r$  columns of the  $n_s \times n_s$  orthogonal matrix  $\mathbf{U}$  identify an orthonormal basis for the  $r$ -dimensional cokernel of  $\mathbf{A}_{\text{DoD}}^{\text{DKM}}(t_p)$ .

For a chosen number  $n_c < r$  of constraints, let us define the  $n_s \times P$  diagonal matrix  $\boldsymbol{\Sigma}^{\text{CE}(n_c)}$  obtained from  $\boldsymbol{\Sigma}$  by setting to zero its diagonal elements with index  $j > n_c$ . By the Eckart–Young theorem of linear algebra, the  $n_s \times P$  matrix

$$\mathbf{A}_{\text{DoD}}^{\text{CE}(n_c)}(t_p) = \mathbf{U} \boldsymbol{\Sigma}^{\text{CE}(n_c)} \mathbf{V}^T \quad (59)$$

represents the “best approximation” to  $\mathbf{A}(t_p)$  that can be achieved by a matrix of rank  $n_c$ , in the sense of minimizing the Frobenius measure  $\delta_{\text{Fro}}$  of the approximation defined by

$$\begin{aligned} \delta_{\text{Fro}}^2(n_c) &= \frac{\left\| \mathbf{A}_{\text{DoD}}^{\text{DKM}}(t_p) - \mathbf{A}_{\text{DoD}}^{\text{CE}(n_c)}(t_p) \right\|_{\text{Fro}}^2}{\left\| \mathbf{A}_{\text{DoD}}^{\text{DKM}}(t_p) \right\|_{\text{Fro}}^2} \\ &= \frac{\sum_{j=1}^{n_s} \sum_{p=1}^P \left[ \Lambda_{\text{DoD},jp}^{\text{DKM}}(t_p) - \Lambda_{\text{DoD},jp}^{\text{CE}(n_c)}(t_p) \right]^2}{\sum_{j=1}^{n_s} \sum_{p=1}^P \left[ \Lambda_{\text{DoD},jp}^{\text{DKM}}(t_p) \right]^2} \end{aligned} \quad (60)$$

which turns out to be equal to the ratio

$$\delta_{\text{Fro}}(n_c) = \frac{\sum_{i=n_c+1}^r \sigma_i}{\sum_{i=1}^r \sigma_i} \quad (61)$$

where  $\sigma_{n_c+1}$  is the first neglected singular value.

The ASVDADD algorithm adopts

$$\epsilon_{\text{ASVDADD}}(n_c) = \delta_{\text{Fro}}^2(n_c) \quad (62)$$

This error measure corresponds to accepting in Eq. (54) the weight function  $w^2(t)$  that has been implicitly chosen by the differential equation solver we used for the DKM simulation so as to

adapt and refine the time discretization grid where the solution changes rapidly.

By construction, the first  $n_c$  columns of the  $n_s \times n_s$  orthogonal matrix  $U$  identify an orthonormal basis for the  $n_c$ -dimensional cokernel of  $A_{\text{DoD}}^{\text{CE}(n_c)}(t_p)$ . This means that, if we denote these columns by  $\mathbf{a}_i^{\text{CE}}$ , we can write

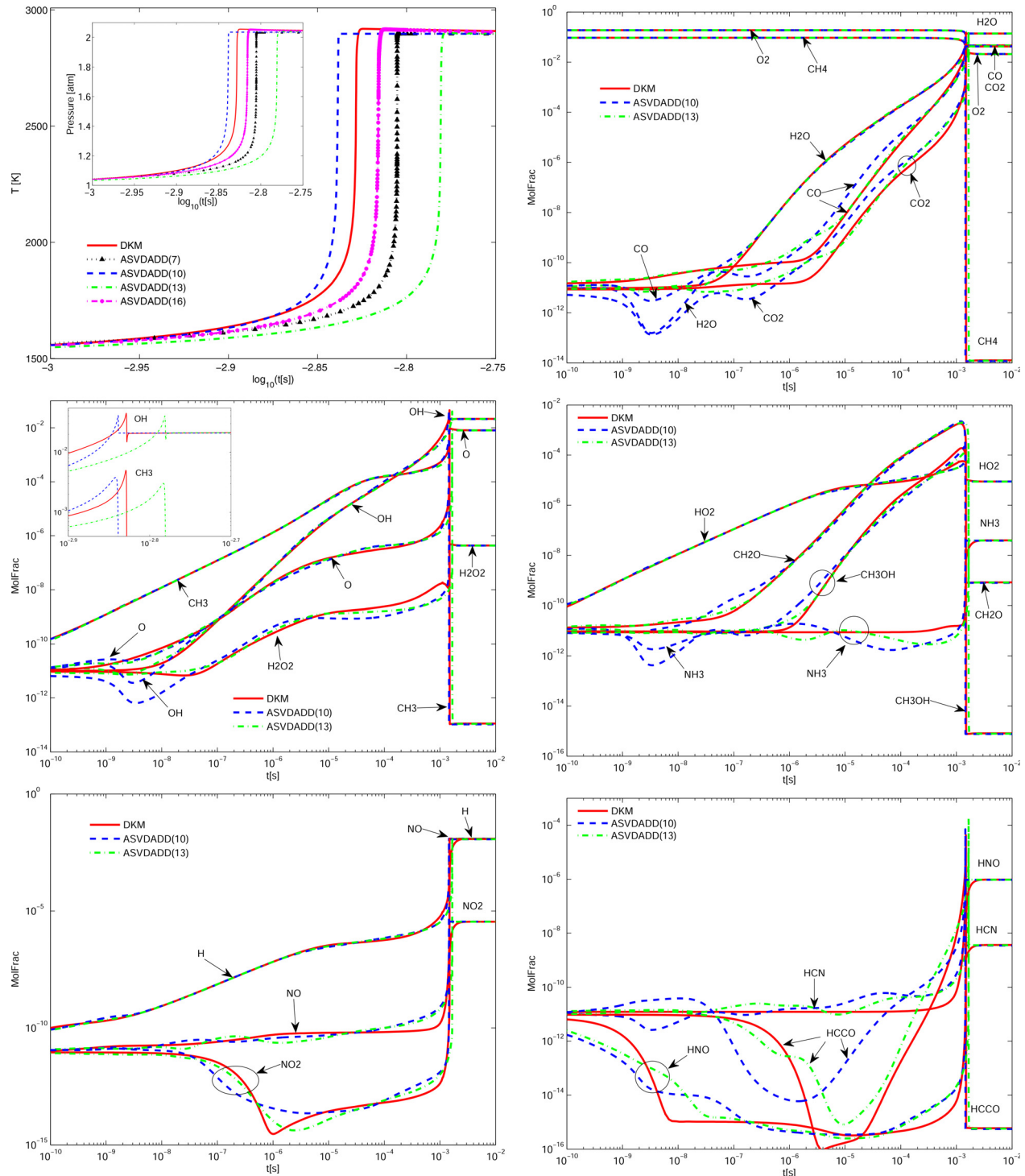


**Fig. 1** Constant- $(E, V)$  ignition of a homogeneous mixture of methane and air. Initially, the mixture is at 1500 K and 1 atm, with 1 mol of  $\text{CH}_4$ , stoichiometric amounts of  $\text{O}_2$ ,  $\text{N}_2$ , and Ar (respectively, 2 mol, 7.52 mol, and 0.08 mol), and very small amounts (between  $10^{-12}/10^{-10}$  mol) for each of the other 49 species. The plots compare temperature, pressure, and mole-fraction time traces obtained from the DKM simulation with those obtained from the RCCE(C) simulations based on  $C = n_c + n_{\text{el}}$  constraints, with  $C = 10$  and 13, of which  $n_{\text{el}} = 5$  are the element conservation ones (C, H, O, N, Ar) and the remaining  $n_c = C - n_{\text{el}}$  are those obtained from the ASVDADD algorithm based on the DoD traces produced by the DKM simulation. To check the robustness of the ASVDADD algorithm, the plots for temperature shows RCCE results also for  $C = 7$  and 16.

$$A_{\text{DoD}}^{\text{CE}(n_c)}(t_p) = \sum_{i=1}^{n_c} \gamma_i^{\text{CE}}(t_p) \mathbf{a}_i^{\text{CE}} \quad (63)$$

thus achieving the objective of the RCCE modeling approximation, because the first  $n_c$  columns of the matrix  $U$  can be taken as

the desired  $n_c$  “best” RCCE constraints  $\mathbf{a}_i^{\text{CE}}$  (in addition to the  $n_{\text{el}}$  elemental ones).

The great advantage of the ASVDADD procedure is that—at the expense of a specific but very natural choice for the measure of “approximation” and hence of “optimality” of the choice of

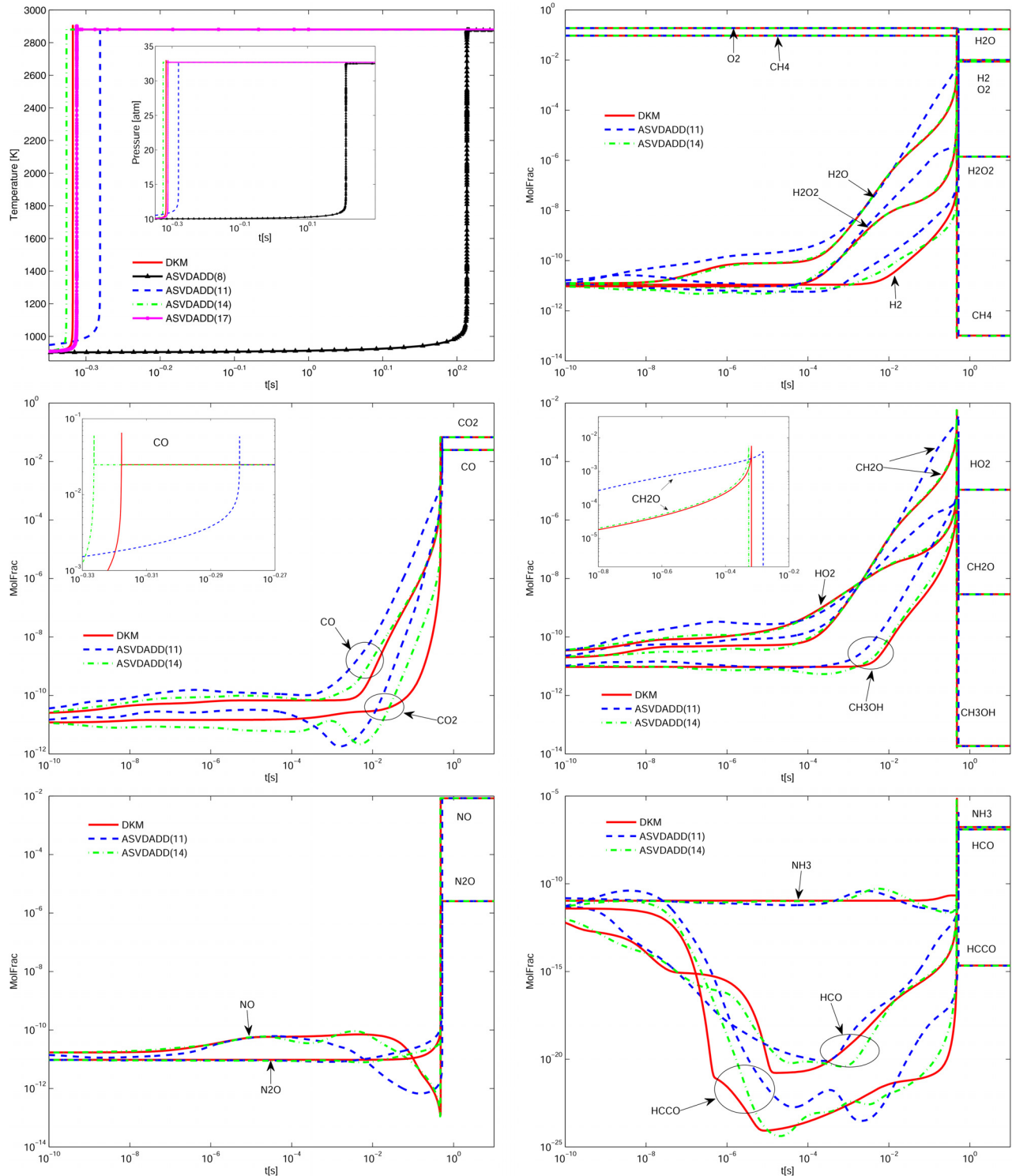


**Fig. 2** Constant- $(E, V)$  ignition of a homogeneous mixture of methane and air. Initially, the mixture is at 900 K and 10 atm, with 1 mol of  $\text{CH}_4$ , stoichiometric amounts of  $\text{O}_2$ ,  $\text{N}_2$ , and Ar (respectively, 2 mol, 7.52 mol, and 0.08 mol), and very small amounts (between  $10^{-12}/10^{-10}$  mol) for each of the other 49 species. The plots compare temperature, pressure and mole-fraction time traces obtained from the DKM simulation with those obtained from the RCCE(C) simulations based on  $C = n_c + n_{\text{el}}$  constraints, with  $C = 11$  and 14, of which  $n_{\text{el}} = 5$  are the element conservation ones (C, H, O, N, Ar) and the remaining  $n_c = C - n_{\text{el}}$  are those obtained from the ASVDADD algorithm based on the DoD traces produced by the DKM simulation. To check the robustness of the ASVDADD algorithm, the plots for temperature shows RCCE results also for  $C = 8$  and 17.

constraints—the SVD of  $A_{\text{DoD}}^{\text{DKM}}(t_p)$  provides at once the entire spectrum of optimal constraints (the first  $r$  columns of  $U$ ) in decreasing order of importance. The optimal set of  $n_c$  constraint vectors  $a_i^{\text{CE}}$  are just the first  $n_c$  columns of  $U$ .

## 7 Validation of the Approximate Singular Value Decomposition of the Actual Degrees of Disequilibrium Method for an Ignition Problem

The present validation study focuses on the ignition of a homogeneous stoichiometric mixture of methane and air in a constant volume and constant energy setup, for two initial conditions, 900 K and 10 atm, and 1500 K and 1 atm. In Ref. [1], a demonstration of the efficiency and robustness of the ASVDADD algorithm was done for a 29 species/133 reactions C1/H/O submechanism [10] of the GRI-Mech 3.0 scheme [22]. Here, instead, to probe the new algorithm in a more complex situation, we retain the full GRI-Mech 3.0 scheme, which considers  $n_r = 325$  reactions between  $n_s = 53$  species with  $n_{\text{el}} = 5$  elements (C, H, O, N, Ar) that includes  $\text{NO}_x$  formation.

From the numerical point of view, considering our limited computational needs, especially the choice of the homogeneous ignition problem which requires no integration with computational fluid dynamics, we opted for the flexibility we could gain by rewriting the entire set of DKM, ASVDADD, and RCCE codes in

MATLAB so as to use the built-in differential equations solvers. In particular, we used the ode15s solver for the integration of the stiff DKM and RCCE system of species balance and energy balance equations.

To avoid infinite values of the DoD's, we set an initial composition  $N_j(0)$  that is not exactly stoichiometric. We assume 1 mol of  $\text{CH}_4$ , stoichiometric amounts of  $\text{O}_2$ ,  $\text{N}_2$ , and Ar (respectively, 2 mol, 7.52 mol, and 0.08 mol), and  $10^{-10}$  mol for each of the other 49 species.

We proceed as follows: We first run a full DKM simulation with these initial amounts and the initial temperature  $T(0)$  and pressure  $p(0)$  of interest (in this study, either 1500 K and 1 atm or 900 K and 10 atm). Clearly, the volume is fixed by  $V = N(0)RT(0)/p(0)$  and so is the energy via the specific heats dependence on temperature. We use the results of the DKM simulation to compute the  $n_s \times P$  matrix  $A_{\text{DoD}}^{\text{DKM}}(t_p)$  where the nonuniform sequence of  $P$  time steps has been chosen by the ode15s solver. We then compute the SVD of this matrix using the svd MATLAB function which returns the  $n_s \times n_s$  orthogonal matrix  $U$  whose columns essentially identify all the ASVDADD constraints to be added to the elemental constraints. Thus, for a chosen value of  $n_c$  we take the first  $n_c$  columns of the matrix  $U$  as the nonelemental constraints,  $a_i^{\text{CE}}$ , additional to the  $n_{\text{el}}$  elemental ones,  $a_i^{\text{EL}}$ . Next, we run the RCCE(C) simulation based on these  $C = n_c + n_{\text{el}}$  constraints. Since, as explained, for example, in

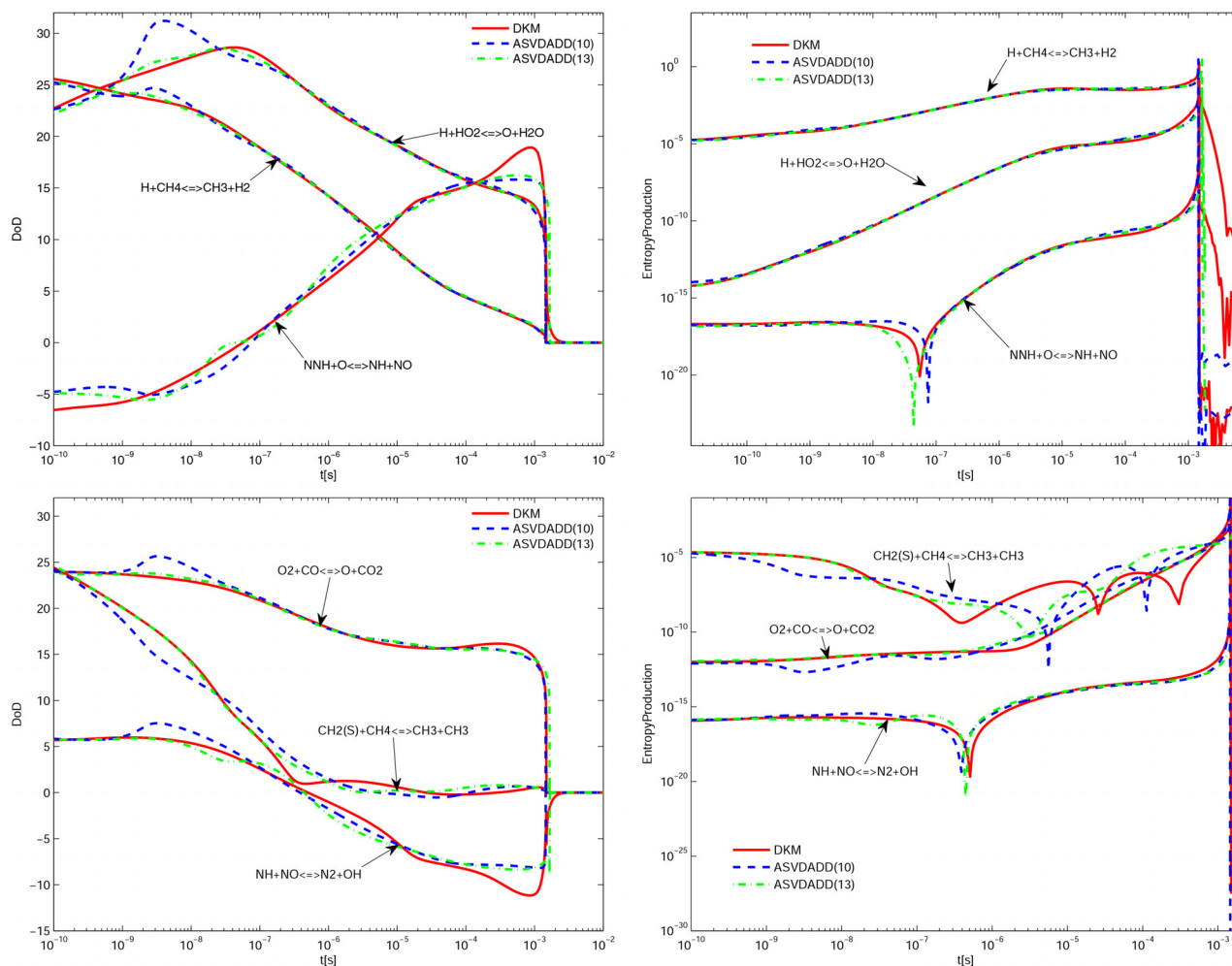


**Fig. 3** Constant- $(E, V)$  ignition of a homogeneous mixture of methane and air. Initially, the mixture is at 1500 K and 1 atm, with 1 mol of  $\text{CH}_4$ , stoichiometric amounts of  $\text{O}_2$ ,  $\text{N}_2$ , and Ar (respectively, 2 mol, 7.52 mol, and 0.08 mol), and very small amounts (between  $10^{-12}/10^{-10}$  mol) for each of the other 49 species. Same simulations as in Fig. 1. The plots compare, for a small sample of reactions, the DoD time traces obtained from the DKM simulation with those obtained from the RCCE(C) simulations based on  $C = n_c + n_{\text{el}}$  constraints, with  $C = 10$  and 13, of which  $n_{\text{el}} = 5$  are the element conservation ones.

Refs. [10–13], it is computationally convenient to solve the rate equations for the  $C$  constraint potentials  $\gamma_i^{\text{EL,CE}}(t)$  and  $\gamma_i^{\text{CE}}(t)$  (rather than for the species concentrations), we need to start the computation by establishing initial values  $\gamma_i^{\text{EL,CE}}(0)$  and  $\gamma_i^{\text{CE}}(0)$  of the constraint potentials that through Eq. (43) approximate well the given initial composition. We do so by imposing Eq.

(43) only for a set of  $C$  “major species,” i.e., by solving the system of  $C$  equations

$$\sum_{i=1}^{n_{\text{el}}} \gamma_i^{\text{EL,CE}}(0) a_{ij}^{\text{EL}} + \sum_{i=1}^{n_c} \gamma_i^{\text{CE}}(0) a_{ij}^{\text{CE}} = \lambda_{jj}(T(0), p(0)) - \ln X_j^{\text{CE}}(0) \quad j = 1, \dots, C \quad (64)$$

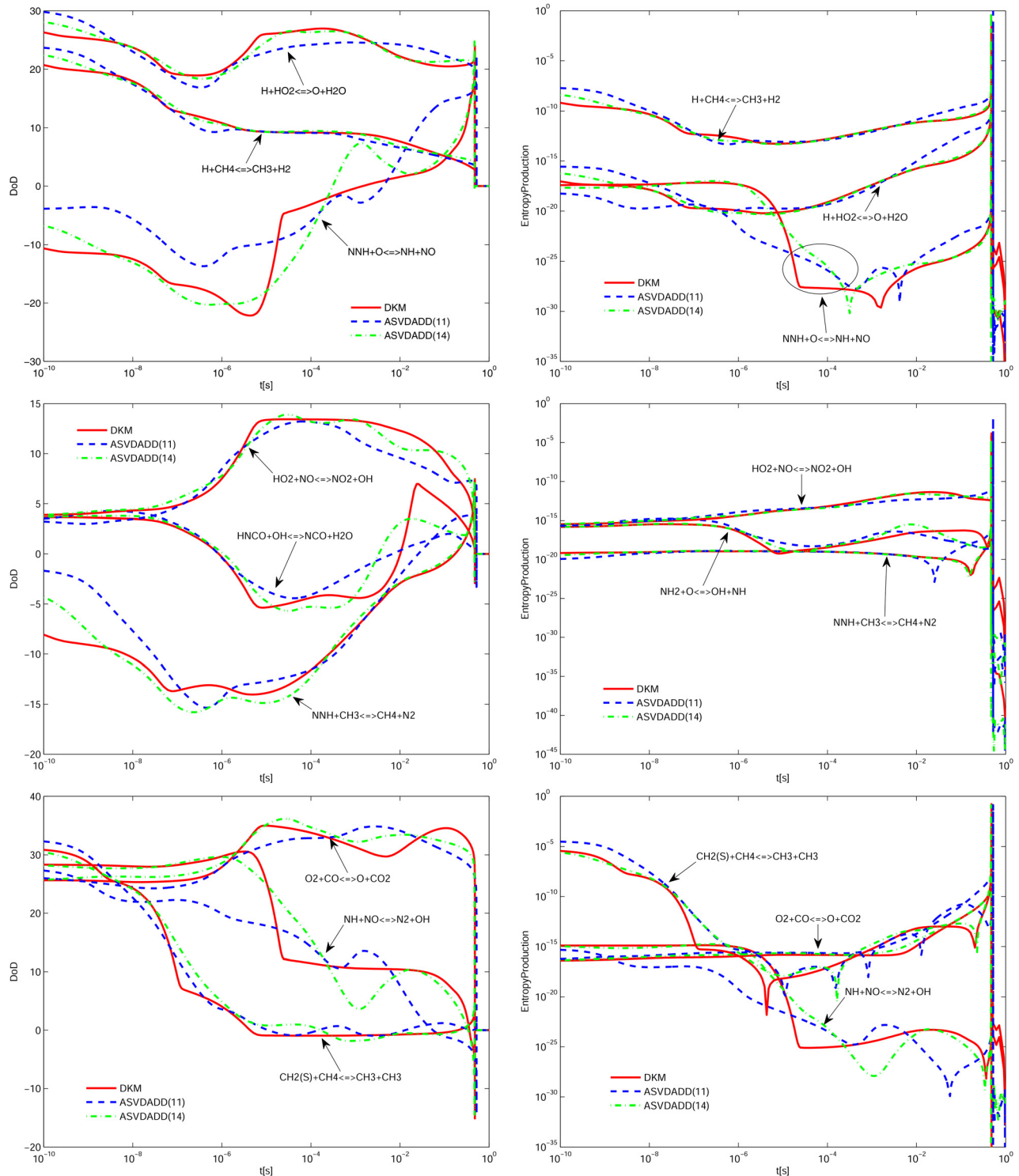


**Fig. 4** Constant- $(E, V)$  ignition of a homogeneous mixture of methane and air. Initially, the mixture is at 900 K and 10 atm, with 1 mol of  $\text{CH}_4$ , stoichiometric amounts of  $\text{O}_2$ ,  $\text{N}_2$ , and Ar (respectively, 2 mol, 7.52 mol, and 0.08 mol), and very small amounts (between  $10^{-12}/10^{-10}$  mol) for each of the other 49 species. Same simulations as in Fig. 2. The plots compare, for a small sample of reactions, the DoD time traces obtained from the DKM simulation with those obtained from the RCCE(C) simulations based on  $C = n_c + n_{\text{el}}$  constraints, with  $C = 11$  and 14, of which  $n_{\text{el}} = 5$  are the element conservation ones.

for the  $C$  unknown values  $\gamma_i^{\text{EL,CE}}(0)$  and  $\gamma_i^{\text{CE}}(0)$ , where we empirically selected as major species the first  $C$  in a list where they are ranked in decreasing order by their values of the sum

$$\left( \sum_{i=1}^{n_{\text{el}}} a_{ij}^{\text{EL}} + \sum_{i=1}^{n_c} a_{ij}^{\text{CE}} \right) \lambda_{jj}(T(0), p(0)) N_j(0) \quad (65)$$

The values  $\gamma_i^{\text{EL,CE}}(0)$  and  $\gamma_i^{\text{CE}}(0)$  are also used, again in Eq. (43), to compute the corrected initial mole fractions  $X_j^{\text{CE}}$  of all the other species and, using  $N = p(0)V/RT(0)$ , the corrected initial amounts  $N_j^{\text{CE}}(0)$ . Finally, we use these corrected initial amounts to run a corrected DKM simulation that we use to compare results with the RCCE( $C$ ) simulations.

The plots in Fig. 1 compare temperature, pressure, and mole-fraction time-traces obtained from the DKM simulation with those obtained, for  $T(0) = 1500$  K and  $p(0) = 1$  atm, from the RCCE( $C$ ) simulations based on  $C = n_c + n_{\text{el}}$  constraints. It is noted that with a relatively small number (5 and 8) of nonelemental constraints, the RCCE results are in very good agreement with the DKM results, even in capturing fine details such as the overshoot/undershoot in the OH concentration at ignition time shown in one of the insets. To check the robustness of the ASVDADD algorithm, the plots for temperature show RCCE results also for  $C = 7$  and 16, showing that to capture well also the temperature overshoot we need 11 nonelemental constraints.

Figure 2 shows similar comparisons for  $T(0) = 900$  K and  $p(0) = 10$  atm.

For a small sample of reactions, Figs. 3 and 4 compare, for the same simulations as in Figs. 1 and 2, respectively, the DoD and entropy production time traces obtained from the DKM simulation with those obtained from the RCCE( $C$ ) simulations.

## 8 Conclusions

The ASVDADD algorithm for systematic RCCE constraint identification is based on analyzing how the DoD of the chemical reactions behave in a full DKM test simulation. Geometrically, the procedure identifies a low-dimensional subspace in DoD space from which the actual DoD traces do not depart beyond a fixed distance related to a preset tolerance level.

The effectiveness and robustness of the methodology have already been demonstrated in Ref. [1] for several test cases of increasing complexity in the framework of oxycombustion of hydrogen (eight species, 24 reactions) and methane (29 species, 133 reactions). In the present paper, we provide a demonstration for the even more complex full GRI-Mech 3.0 kinetic scheme (53 species, 325 reactions) for methane/air combustion including nitrogen oxidation.

The excellent performance of the ASVDADD constraints confirm that conclusion in Ref. [1] that the new algorithm essentially resolves the difficulties [23,24] that have prevented the RCCE method from a more widespread use in model order reduction of detailed combustion kinetic models of hydrocarbon fuels.

In future work, we will show that the same model order reduction logic can find natural extensions also in the more general field of nonequilibrium thermodynamics, in particular in the general frameworks discussed in Refs. [25] and [26].

## References

[1] Beretta, G. P., Janbozorgi, M., and Metghalchi, H., 2016, "Degree of Disequilibrium Analysis for Automatic Selection of Kinetic Constraints in the

Rate-Controlled Constrained-Equilibrium Method," *Combust. Flame*, **168**, pp. 342–364.

[2] Keck, J. C., and Gillespie, D., 1971, "Rate-Controlled Partial-Equilibrium Method for Treating Reacting Gas Mixtures," *Combust. Flame*, **17**(2), pp. 237–241.

[3] Keck, J. C., 1979, "Rate-Controlled Constrained Equilibrium Method for Treating Reactions in Complex Systems," *The Maximum Entropy Formalism*, R. D. Levine and M. Tribus, eds., MIT Press, Cambridge, MA, pp. 219–245.

[4] Beretta, G. P., and Keck, J. C., 1986, "The Constrained-Equilibrium Approach to Nonequilibrium Dynamics," *Second Law Analysis and Modeling*, Vol. 3, R. A. Gaggioli, ed., ASME, New York, pp. 135–139.

[5] Law, R., Metghalchi, M., and Keck, J. C., 1989, "Rate-Controlled Constrained Equilibrium Calculations of Ignition Delay Times in Hydrogen-Oxygen Mixtures," *Symp. (Int.) Combust.*, **22**(1), pp. 1705–1713.

[6] Keck, J. C., 1990, "Rate-Controlled Constrained-Equilibrium Theory of Chemical Reactions in Complex Systems," *Prog. Energy Combust. Sci.*, **16**(2), pp. 125–154.

[7] Bishnu, P., Hamiroune, D., Metghalchi, H., and Keck, J. C., 1997, "Constrained-Equilibrium Calculations for Chemical Systems Subject to Generalized Linear Constraints Using the NASA and STANJAN Equilibrium Programs," *Combust. Theory Modell.*, **1**(3), pp. 295–312.

[8] Hamiroune, D., Bishnu, P., Metghalchi, H., and Keck, J. C., 1998, "Rate-Controlled Constrained-Equilibrium Method Using Constraint Potentials," *Combust. Theory Modell.*, **2**(1), pp. 81–94.

[9] Yousefian, V., 1998, "A Rate-Controlled Constrained-Equilibrium Thermochemistry Algorithm for Complex Reacting Systems," *Combust. Flame*, **115**(1–2), pp. 66–80.

[10] Janbozorgi, M., Ugarte, S., Metghalchi, H., and Keck, J. C., 2009, "Combustion Modelling of Mono-Carbon Fuels Using the Rate-Controlled Constrained-Equilibrium Method," *Combust. Flame*, **156**(10), pp. 1871–1885.

[11] Beretta, G. P., Keck, J. C., Janbozorgi, M., and Metghalchi, H., 2012, "The Rate-Controlled Constrained-Equilibrium Approach to Far-From-Local-Equilibrium Thermodynamics," *Entropy*, **14**(2), pp. 92–130.

[12] Janbozorgi, M., and Metghalchi, H., 2012, "Rate-Controlled Constrained-Equilibrium Modeling of H-O Reacting Nozzle Flow," *J. Propul. Power*, **28**(4), pp. 677–684.

[13] Nicolas, G., Janbozorgi, M., and Metghalchi, H., 2014, "Constrained-Equilibrium Modeling of Methane Oxidation in Air," *ASME J. Energy Resour. Technol.*, **136**(3), p. 032205.

[14] Nicolas, G., and Metghalchi, H., 2015, "Comparison Between RCCE and Shock Tube Ignition Delay Time at Low Temperatures," *ASME J. Energy Resour. Technol.*, **137**(6), p. 062203.

[15] Gyftopoulos, E. P., and Beretta, G. P., 2005, *Thermodynamics: Foundations and Applications*, Dover Publications, Mineola, NY.

[16] Beretta, G. P., and Gyftopoulos, E. P., 2015, "What Is a Chemical Equilibrium State?," *ASME J. Energy Resour. Technol.*, **137**(2), p. 021008.

[17] Beretta, G. P., and Gyftopoulos, E. P., 2004, "Thermodynamic Derivations of Conditions for Chemical Equilibrium and of Onsager Reciprocal Relations for Chemical Reactors," *J. Chem. Phys.*, **121**(6), pp. 2718–2728.

[18] Beretta, G. P., 2009, "Nonlinear Quantum Evolution Equations to Model Irreversible Adiabatic Relaxation With Maximal Entropy Production and Other Nonunitary Processes," *Rep. Math. Phys.*, **64**(1–2), pp. 139–168.

[19] Hiremath, V., Ren, Z., and Pope, S. B., 2011, "Combined Dimension Reduction and Tabulation Strategy Using ISAT-RCCE-GALI for the Efficient Implementation of Combustion Chemistry," *Combust. Flame*, **158**(1), pp. 2113–2127.

[20] Martin, C. D., and Porter, M. A., 2012, "The Extraordinary SVD," *Am. Math. Mon.*, **119**(10), pp. 838–851.

[21] Wold, S., Esbensen, K., and Geladi, P., 1987, "Principal Component Analysis," *Chemom. Intell. Lab. Syst.*, **2**(1–3), pp. 37–52.

[22] Smith, G. P., Golden, D. M., Frenklach, M., Moriarty, N. W., Eiteneer, B., Goldenberg, M., Bowman, C. T., Hanson, R. K., Song, S., Gardiner, W. C., Jr., Lissianski, V. V., and Qin, Z., 2017, "GRI-Mech 3.0," accessed Nov. 17, 2017, <http://combustion.berkeley.edu/gri-mech/version30/text30.html>

[23] Nicolas, G., and Metghalchi, H., 2016, "Development of the Rate-Controlled Constrained-Equilibrium Method for Modeling of Ethanol Combustion," *ASME J. Energy Resour. Technol.*, **138**(2), p. 022205.

[24] Hadi, F., Janbozorgi, M., Sheikhi, R., and Metghalchi, H., 2016, "A Study of Interactions Between Mixing and Chemical Reaction Using the Rate-Controlled Constrained-Equilibrium Method," *J. Non-Equilib. Thermodyn.*, **41**(4), pp. 257–278.

[25] Beretta, G. P., 2014, "Steepest Entropy Ascent Model for Far-Nonequilibrium Thermodynamics: Unified Implementation of the Maximum Entropy Production Principle," *Phys. Rev. E*, **90**, p. 042113.

[26] Montefusco, A., Consonni, F., and Beretta, G. P., 2015, "Essential Equivalence of the General Equation for the Nonequilibrium Reversible-Irreversible Coupling (GENERIC) and Steepest-Entropy-Ascent Models of Dissipation for Nonequilibrium Thermodynamics," *Phys. Rev. E*, **91**(4), p. 042138.